BOREAL ENVIRONMENT RESEARCH 20: 679–692
ISSN 1239-6095 (print) ISSN 1797-2469 (online)

Helsinki 18 December 2015

Temporal and spatial carbon dioxide concentration patterns in a small boreal lake in relation to ice-cover dynamics

Blaize A. Denfeld[1)]*, Marcus B. Wallin[1)2)], Erik Sahlée[2)], Sebastian Sobek[1)], Jovana Kokic[1)], Hannah E. Chmiel[1)] and Gesa A. Weyhenmeyer[1)]

[1)] *Department of Ecology and Genetics/Limnology, Uppsala University, Norbyvägen 18D, SE-752 36 Uppsala, Sweden (*corresponding author's e-mail: blaize.denfeld@ebc.uu.se)*
[2)] *Department of Earth Sciences, Uppsala University, Villavägen 16, SE-752 36 Uppsala, Sweden*

Received 1 Dec. 2014, final version received 4 May. 2015, accepted 4 May. 2015

Denfeld B.A., Wallin M.B., Sahlée E., Sobek S., Kokic J., Chmiel H.E. & Weyhenmeyer G.A. 2015: Temporal and spatial carbon dioxide concentration patterns in a small boreal lake in relation to ice-cover dynamics. *Boreal Env. Res.* 20: 679–692.

Global carbon dioxide (CO_2) emission estimates from inland waters commonly neglect the ice-cover season. To account for CO_2 accumulation below ice and consequent emissions into the atmosphere at ice-melt we combined automatically-monitored and manually-sampled spatially-distributed CO_2 concentration measurements from a small boreal ice-covered lake in Sweden. In early winter, CO_2 accumulated continuously below ice, whereas, in late winter, CO_2 concentrations remained rather constant. At ice-melt, two CO_2 concentration peaks were recorded, the first one reflecting lateral CO_2 transport within the upper water column, and the second one reflecting vertical CO_2 transport from bottom waters. We estimated that 66%–85% of the total CO_2 accumulated in the water below ice left the lake at ice-melt, while the remainder was stored in bottom waters. Our results imply that CO_2 accumulation under ice and emissions at ice-melt are more dynamic than previously reported, and thus need to be more accurately integrated into annual CO_2 emission estimates from inland waters.

Introduction

Inland waters play an important role in the global carbon cycle, receiving, transporting and processing carbon and emitting carbon dioxide (CO_2) and methane (CH_4) into the atmosphere (Battin *et al*. 2009). Several global CO_2 emission estimates from lakes and streams are available (Cole *et al*. 2007, Tranvik *et al*. 2009, Aufdenkampe *et al*. 2011) with temporal, in particular seasonal variations, based on simple assumptions rather than evidence. Most of the lakes in the northern hemisphere are however covered by ice during substantial parts of the year (Weyhenmeyer *et al*. 2011) where ice acts as a barrier to atmospheric exchange causing high concentrations of CO_2 to accumulate in lakes (Striegl and Michmerhuizen 1998, Kortelainen *et al*. 2006). Most commonly global lake CO_2 emission estimates compensate for CO_2 accumulation (i.e. the lack of CO_2 emitted) during the ice-cover period by assuming that a rapid outburst of CO_2 to the atmosphere at ice-melt accounts for all the CO_2 that has accumulated during winter (Cole *et al*. 2007). More recently, Butman and Raymond (2011) attempted to account for the ice-cover period of running waters by calculating annual CO_2 emissions for the open-water season only.

Editor in charge of this article: Harri Koivusalo

Raymond *et al*. (2013) offered another approach in the currently most comprehensive estimate of CO_2 emissions from global inland waters. They discounted periods during which running waters were ice-covered from the emission calculations, while they assumed linear accumulation of CO_2 under the ice followed by complete and rapid emission at ice-out for lakes and reservoirs (Raymond *et al*. 2013). However, all these methods neglect the dynamics and importance of under ice CO_2 accumulation and CO_2 outburst at spring ice-melt, which in lakes can be substantial: Karlsson *et al*. (2013), for example, estimated that up to 56% of the total annual CO_2 emission can occur at ice-melt alone. Such estimates are, however, based on manual samples that do not capture CO_2 dynamics at an hourly and daily time scales. Since CO_2 emission at ice-melt can occur within days (Huotari *et al*. 2009), improved estimates of CO_2 emissions during this period are needed.

It is well established that lakes are supersaturated with CO_2 caused by net heterotrophy, where respiration exceeds primary production (Cole *et al*. 1994). Moreover, high CO_2 accumulation in lakes under ice has been attributed to respiration of terrestrial organic-carbon inputs (Striegl *et al*. 2001) and of organic carbon produced by benthic algae the previous summer (Karlsson *et al*. 2008). In addition to respiration, variations in lake water CO_2 are a result of photosynthesis, photo-transformation, methane oxidation, catchment contribution and water column mixing. To some extent, ice and snow-cover dynamics alter these processes, preventing atmospheric inputs and gas exchange (Striegl *et al*. 2001), limiting solar radiation (Belzile *et al*. 2001), and reducing the effect of turbulent heat flux on lake mixing (Rouse *et al*. 2005). Thus, the seasonal dynamics of snow and ice cover greatly influences the magnitude of these mechanisms (Gunn and Keller 1985), which consequently may lead to spatial and temporal variations in lake water CO_2 during the ice-cover period.

One way to improve estimates of CO_2 emissions is to increase the frequency of CO_2 measurements (Sellers *et al*. 1995). Recent advancements in technology have allowed for the development of *in situ* CO_2 sensors (e.g. Johnson *et al*. 2010). However, at present, only a very limited number of *in situ* continuous CO_2 measurements under ice and at ice-melt are available for lakes and reservoirs (Baehr and DeGrandpre 2002, 2004, Huotari *et al*. 2009, Demarty *et al*. 2011). These studies highlight the complexity of CO_2 dynamics at ice-melt but are limited in their ability to account for the spatial variability of CO_2 across the entire lake or reservoir basin. A recent study by Schilder *et al*. (2013) suggests that surface water CO_2 concentrations during the open-water period can vary across the lake. Additionally, CO_2 concentrations can vary vertically in the lake during stratification periods, with CO_2-rich bottom waters contributing to high CO_2 emission during turnover periods (Kortelainen *et al*. 2006). Thus, in order to improve the accuracy of CO_2 emission estimates, during the understudied ice-melt period, continuous CO_2 concentration measurements should be combined with spatially distributed CO_2 concentration measurements in ice-covered lakes.

This study aimed to explore the current assumptions global CO_2 emission estimates make for ice-covered lakes, i.e. that CO_2 accumulates linearly under ice and that at ice-melt all CO_2 that has been accumulated is rapidly emitted into the atmosphere. Further, we aimed to quantify the spatial and temporal variability of CO_2 in lake water from ice-on to ice-off. We hypothesized that (1) CO_2 accumulates linearly under ice during the whole winter, (2) CO_2 accumulates faster in bottom than in surface waters, and finally (3) the amount of CO_2 that is emitted to the atmosphere at ice-melt is comparable to the amount of CO_2 that has been accumulated during the winter.

Methods

Study area

To test our hypotheses we sampled Lake Gäddtjärn, a small boreal lake (6.8 ha) located in mid-Sweden (59.86°N, 15.18°E) with a maximum depth of 10 m, mean depth of 3.8 m, and a volume of 260 000 m^3 at an altitude of 254 m a.s.l. The lake has two main inlets, which drain a catchment area of 226 ha comprising 84% boreal forest, 12% wetlands and 4% water (draining three very small headwater lakes). About 20%

of the total catchment area drains directly into the lake, while 80% drains via two streams (Kokic *et al*. 2015). The lake has a theoretical water residence time of ~2 months (calculated as mean discharge at the outlet divided by the lake volume) and drains into a larger lake further downstream. According to the Swedish Meteorological and Hydrological Institute, the long-term mean (1961–1990) annual temperature is 4.5 °C and annual precipitation is 900 mm. Ice formation usually begins in mid-November to early December and ice-melts in mid-April. Six sampling sites on the lake were chosen to represent varying lake depths from 1.4 to 9.5 m (Fig. 1).

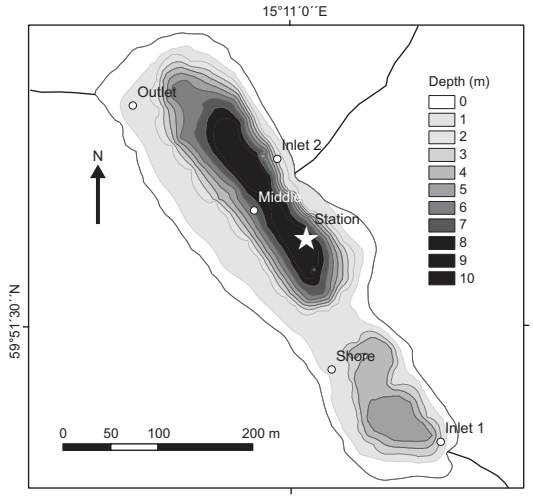

Fig. 1. Sampling locations in Lake Gäddtjärn. The star indicates the station site where CO_2 concentrations (shown in Fig. 2), dissolved oxygen, pH, water temperature and light intensity were monitored automatically and where the CO_2 vertical profile sampling was carried out.

Continuous measurements

We automatically monitored CO_2 concentration (μM), dissolved oxygen (DO, mg l^{-1}), pH, water temperature (°C) and light intensity (lux) above the deepest basin of the lake (depth of 9.5 m), during the ice-cover and ice-melt periods between 22 Jan. and 7 May 2013. Hourly partial pressure of CO_2 (p_{CO2}) was measured (and converted into CO_2 concentration) using the Submersible Autonomous Moored Instrument for CO_2 (Sunburst Sensors, SAMI2) suspended in the water column at 2 m depth. SAMI2 was factory calibrated towards NIST (National Institute of Standards and Technology) traceable NDIR (Nondispersive Infrared Sensor) and has an accuracy of ±3 μatm and precision < 1 μatm. We applied correction factors supplied by sunburst sensors when calculating CO_2 concentration, since our CO_2 measurements (mean 2800 μatm) surpassed the NIST-approved validity range of calibration (300–1300 μatm). DO and pH were measured hourly with an autonomous sonde (YSI, Model 6600V2-03; ROX DO probe, Model 6450 AF) suspended at 4 m depth (deployed as part of a separate project). Light intensity was measured hourly with a pendant light logger (HOBO, Model UA-002-64) attached to the top of a subsurface float placed 0.1 m below the surface water. Water temperature was recorded every 4 hours at every meter throughout the total depth of the water column (9 m) with temperature loggers (onset HOBO, Model Pro V2).

Manual measurements

In addition to automatic measurements, between 13 Dec. 2012 and 7 May 2013, we collected water samples five times during the ice-on and once at ice-off. Water was collected using a Ruttner water sampler from five surface-water sites (sampled at 0.5 m) and one vertical profile site (sampled at 0.5, 2, 4, 6 and 8 m depth) located at the deepest point of the lake (Fig. 1). Bubble-free water was drained from the Ruttner into a 60 ml polypropylene syringe and a 12 ml glass vial, for CO_2 and dissolved inorganic carbon (DIC) analyses, respectively. Additional water was collected for dissolved organic carbon (DOC) analysis. All water samples were stored dark and cool until analyzed. Further, at each location, temperature, DO and specific conductivity were measured using an HQ40d Portable Multi-parameter sonde (HACH). Upon returning from the field, water samples for DOC were filtered through a precombusted 0.7 μm Whatman GF/F glass fiber filter. A total carbon analyzer (Sievers 900) equipped with a membrane-based conductivity detector was used to measure DOC and DIC. For each water sample, DOC and DIC were reported as means of three measurements

taken by the total carbon analyzer. DIC and DOC samples were analyzed within two and seven days of sampling, respectively. CO_2 measurements were made immediately upon returning from the field using the headspace equilibration technique, where 40 ml of water was replaced with ambient air and equilibrated with the lake water by vigorously shaking. p_{CO2} of the extracted headspace gas phase and ambient air were measured with a portable infrared gas analyzer (IRGA) (EGM-4, PP Systems Inc, USA) which has an accuracy of < 1% of the calibration range (0–5000 μatm). Headspace p_{CO2} was taken as the average of three measurements and CO_2 concentration was calculated according to Henry's law presented by Weiss (1974) correcting for temperature and the amount of CO_2 added to the syringe by the ambient air (e.g. Sobek *et al*. 2003, Demarty *et al*. 2011, Karlsson *et al*. 2013).

Using manually sampled CO_2 from the vertical profile site, i.e. above the deepest point of the lake, we quantified temporal changes in CO_2 concentrations (ΔCO_2, μM d^{-1}) for 0.5 m (surface water) and at 8 m (bottom water). We received a rate of change by taking the CO_2 concentration difference between sampling occasions divided by the number of days between the sampling. ΔCO_2 was calculated for the early winter (13 Dec. 2012–4 Feb. 2013), late winter (4 Feb.–15 Apr.), and the ice-melt (15 Apr.–7 May) periods. We also estimated whole-lake CO_2 accumulation and loss rates (r, mol CO_2 d^{-1}) by considering the whole-lake CO_2 storage (CS, mol CO_2). CS was calculated as the sum of the measured CO_2 depth profile integrated with the volume of each corresponding depth layer (Michmerhuizen *et al*. 1996). Lake volume at each depth was obtained by digitizing lake contour maps for each 1 m depth. Whole-lake r was then calculated as:

$$r = \frac{CS_{t_2} - CS_{t_1}}{n}, \quad (1)$$

where CS is the whole-lake CO_2 storage at sampling time t, and n is the number of days between sampling occasions t_1 and t_2. Positive values of r indicate CO_2 accumulation in the lake while negative ones CO_2 loss from the lake.

The relative amount of CO_2 accumulated under ice that was released during spring melt ($C_{release}$, %) was calculated as:

$$C_{reselase} = \frac{CS_L}{CS_A} = \frac{CS_{last\ ice} - CS_{no\ ice}}{CS_{last\ ice} - CS_{first\ ice}}, \quad (2)$$

where CS_L is the amount of CO_2 leaving the lake during the ice-off season, CS_A is the amount of CO_2 accumulated in the lake during the sampling period below the ice cover, $CS_{first\ ice}$ is the CS on 13 Dec., $CS_{last\ ice}$ is the CS on 11 Mar., and $CS_{no\ ice}$ is the CS on 7 May.

Since sampling began after the ice had been formed and we did not capture the exact time of ice-off we also made an estimate of $C_{release}$ for the whole ice-cover period by accounting for the full duration of the ice cover. We assumed ice-on to occur on the lake after air temperatures below 0 °C persisted for four consecutive days, corresponding to 28 Nov. 2012. We further assumed ice-off to begin on 15 Apr. 2013, corresponding to a sudden and apparent increase in continuously-measured underwater light conditions. Thus, $CS_{first\ ice}$ was the CS on 28 Nov., calculated as the CS on 13 Dec. minus early winter whole-lake r (13 Dec. 2012–4 Feb. 2013) times 15 days (28 Nov. 2012–13 Dec. 2013). $CS_{last\ ice}$ was the CS on 15 Apr., calculated as the CS on 11 Mar. plus late winter whole-lake r (4 Feb.–15 Apr.) times 35 days (11 Mar.–15 Apr.).

CO_2 emission at ice-melt

Continuous CO_2 concentrations were used to estimate CO_2 emission (CO_{2_E}, mmol m^{-2} d^{-1}) during ice-melt using the following equation:

$$CO_{2_E} = k_{CO_2} \times (CO_{2_w} - CO_{2_a}), \quad (3)$$

where k_{CO_2} is the gas transfer velocity (cm h^{-1}) and (CO_{2_w} – CO_{2_a}) accounts for the difference between CO_2 concentrations in the water and in the air. CO_{2_w} was measured with the SAMI2 instrument at 2 m depth below the surface. CO_{2_a} was set to 406 μatm, the average ambient atmospheric p_{CO2} manually measured at the lake. To account for the difference between CO_2 concentrations just below the water surface we applied a correction factor of –19% to the continuous CO_2 concentration measurements made with the SAMI2 instrument at 2 m depth. This correction is based on the observed CO_2 concentration

difference between 0.5 m and 2 m during the ice-melt period (7 May). The correction results in lower CO_2 concentrations at the water–atmosphere interface, thus our CO_2 emission estimates are conservative. k_{CO_2} was estimated from k_{600} normalized to a temperature-dependent Schmidt number for CO_2 (600 at 20 °C) according to Jähne *et al*. (1987). k_{600} was derived from wind speed based on the relationship from Cole and Caraco (1998). Since the Cole and Caraco (1998) model was based on measurements from a small, wind-sheltered lake comparable to ours, it is well suited to estimate CO_2 emission for this study. Hourly wind speed data were acquired from the nearby meteorological station Kloten site A (59.52°N, 15.15°E). In addition, for validation purposes, k_{600} was also estimated using 6 floating chambers which were placed in the lake to measure k_{600} on 7 May 2013 (Krenz 2013). The floating chamber derived k_{600} for the lake ranged from 1.9 to 4.2 cm h^{-1} with a median of 2.3 cm h^{-1}, and the Cole and Caraco (1998) model for the same day corresponded to an estimated median k_{600} of 2.4 cm h^{-1} and range from 2.1 to 3.1 cm h^{-1}. Thus, the two k_{600} estimates agreed relatively well. To avoid overestimation of k_{600} at high wind speeds we set the wind speed derived k_{600} to a maximum threshold of 4.2 cm h^{-1} since this was the maximum k_{600} directly measured with floating chambers; again, by doing so we calculate a conservative CO_2 emission estimate. The mean ± standard deviation (SD) were calculated for k_{600}, CO_2 and CO_{2_E}.

Statistical analyses

To test whether CO_2 concentrations below the ice cover significantly increased or not we applied a Mann-Kendall trend test, based on the non-normally distributed daily mean CO_2 concentration data from the continuous measurements (Shapiro-Wilk's test result: $p < 0.0001$, $n = 84$). We considered an increase or decrease as significant at $p < 0.05$. We also used the Mann-Kendall trend test to quantify the rate of change in the CO_2 concentration below ice (in days) by calculating the Theil slopes for different periods.

To investigate whether CO_2 accumulates in the bottom water we compared the manually–measured CO_2 concentrations from the bottom water (8 m water depth) at the continuous CO_2 measuring site (site Station in Fig. 1) with the ones from the surface water (0.5 m water depth). Surface and bottom water samples at this site were manually taken on six occasions (13 Dec., 22 Jan., 4 Feb., 26 Feb., 11 Mar. and 7 May). Since the CO_2 data in both the surface and bottom water were normally distributed (Shapiro-Wilk's test result: $p > 0.05$, $n = 6$ for both surface and bottom water) we applied a matched-pairs *t*-test where surface and bottom water CO_2 concentration was paired for each sampling occasion.

Finally, we tested whether there were horizontal CO_2 concentration differences in surface waters below the ice cover, i.e. from December to March. For the test we used a two-way analysis of variance (ANOVA) where we set site (six sites: Inlet1, Inlet 2, Middle, Outlet, Shore and Station) and time (five sampling occasions: 13 Dec. 2012, and 22 Jan., 4 Feb., 26 Feb. and 11 Mar. 2013) as the two independent variables and CO_2 concentration in surface waters at the six sites from December to March as the dependent variable. The CO_2 concentration in surface waters at the six sites from December to March was normally distributed (Shapiro-Wilk's test result: $p > 0.05$, $n = 30$). All statistical tests were performed in JMP version 11.0.0.

Results

Hourly surface-water CO_2 patterns

The surface-water (2 m depth) CO_2 concentration (continuous measurements) change comprised four distinct phases between ice-on and ice-off: an increase from 22 Jan. to 9 Feb., rather constant concentrations from 10 Feb. to 15 Apr., and two peaks after 15 Apr. (Fig. 2). During 22 Jan.–9 Feb., the ice cover steadily built up, and surface water CO_2 concentrations rapidly and significantly increased by 3 μM d^{-1} (Mann-Kendall test: $\tau = 3$, $p < 0.01$, $n = 19$). This increase continued until the ice reached its maximum thickness in early February (Table 1 and Fig. 2). Surface-water CO_2 concentration reached a maximum of 187 μM on 9 Feb. and plateaued thereafter until ice-melt began on

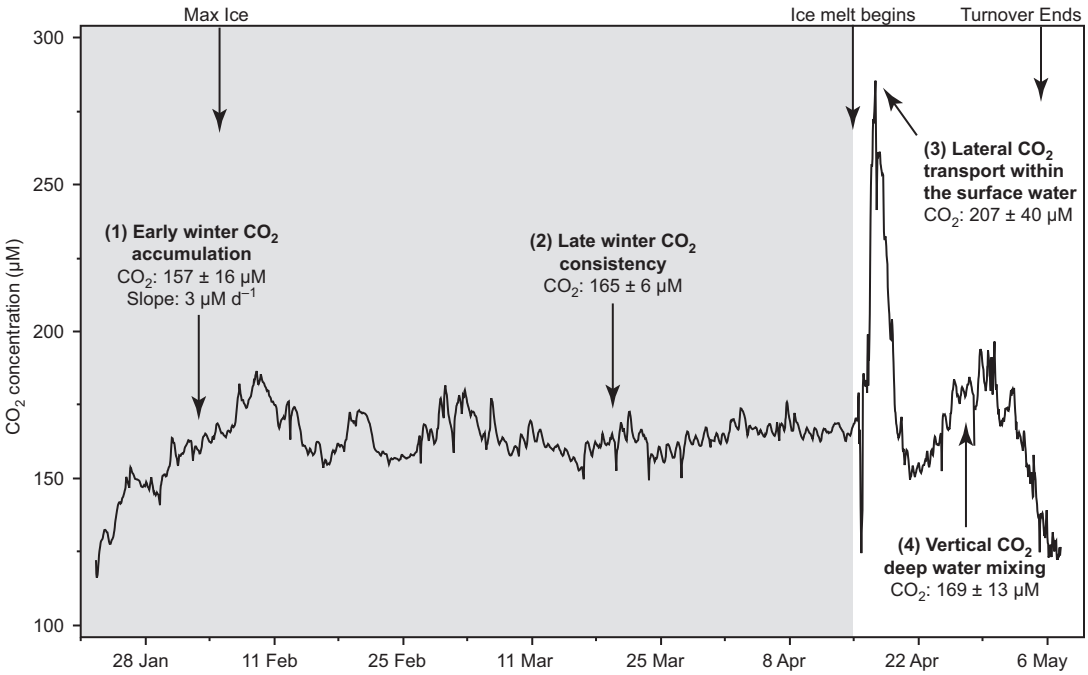

Fig. 2. Automatically-monitored hourly surface-water (2 m) CO_2 concentrations measured during the ice-cover (grey) and ice-melt periods (white) above the deepest site (station site) in Lake Gäddtjärn between 22 Jan. and 7 May 2013. CO_2 concentrations are reported as factory-corrected values. For each period mean ± SD is reported. For the first, period the Theil slope indicating change over time is reported.

15 Apr. During this period (10 Feb.–15 Apr.), surface-water CO_2 concentrations did not show a significant change (Mann-Kendall test: τ = –0.008, p = 0.85, n = 65). As ice-melt began (16 Apr.–20 Apr.), surface-water CO_2 concentrations rapidly increased within only two days from 179 μM to 286 μM (on 17 Apr.), which corresponded to an apparent increase in light intensity (Fig. 3C), and was followed by an equally rapid decline to 157 μM within the next two days. This steep first CO_2 concentration peak was followed by a more gradual CO_2 concentration peak (21 Apr.–4 May) of 197 μM on 30 Apr., followed by a decline to 137 μM within four days (Fig. 2).

Table 1. Ice and snow conditions on the lake, water temperature and chemistry measured at spatially-sampled surface-water sites (Fig. 1, n = 6). Mean ± SD for each sampling date is reported. Whole-lake CO_2 storage (CS) was estimated from integrating CO_2 depth profiles (*see* Methods); m.d. = missing data, n.a. = not applicable.

	13 Dec.	22 Jan.	4 Feb.	26 Feb.	11 Mar.	7 May
Ice thickness (cm)	16 ± 2	27 ± 8	46 ± 14	35 ± 4	46 ± 13	n.a.
Snow depth on ice (cm)	m.d.	m.d.	4 ± 1	14 ± 3	17 ± 2	n.a.
Water temp (°C)	0.1 ± 0	0.2 ± 0.1	0.9 ± 0.9	0.5 ± 0.3	0.3 ± 0.3	12 ± 0.8
Conductivity (μS cm^{-1})	11.7 ± 5.8	19.6 ± 5.3	20.8 ± 4.4	21.4 ± 0.7	21.8 ± 0.6	17.7 ± 0.2
DO (mg l^{-1})	m.d.	13.2 ± 0.0	12.2 ± 1.0	12.4 ± 0.4	12.4 ± 0.8	9.9 ± 0.1
DOC (mg l^{-1})	14.3 ± 0.6	12.2 ± 1.1	12.2 ± 0.8	11.9 ± 1.2	11.2 ± 0.5	12.0 ± 0.1
DIC (mg l^{-1})	1.1 ± 0.1	1.5 ± 0.2	1.8 ± 0.3	1.9 ± 0.2	2. 3 ± 0.3	1.4 ± 0
CO_2 (μM)	102 ± 10	145 ± 27	183 ± 30	162 ± 22	189 ± 24	113 ± 8
Whole-lake CS (mol)	27938	36116	45856	42844	45905	30618

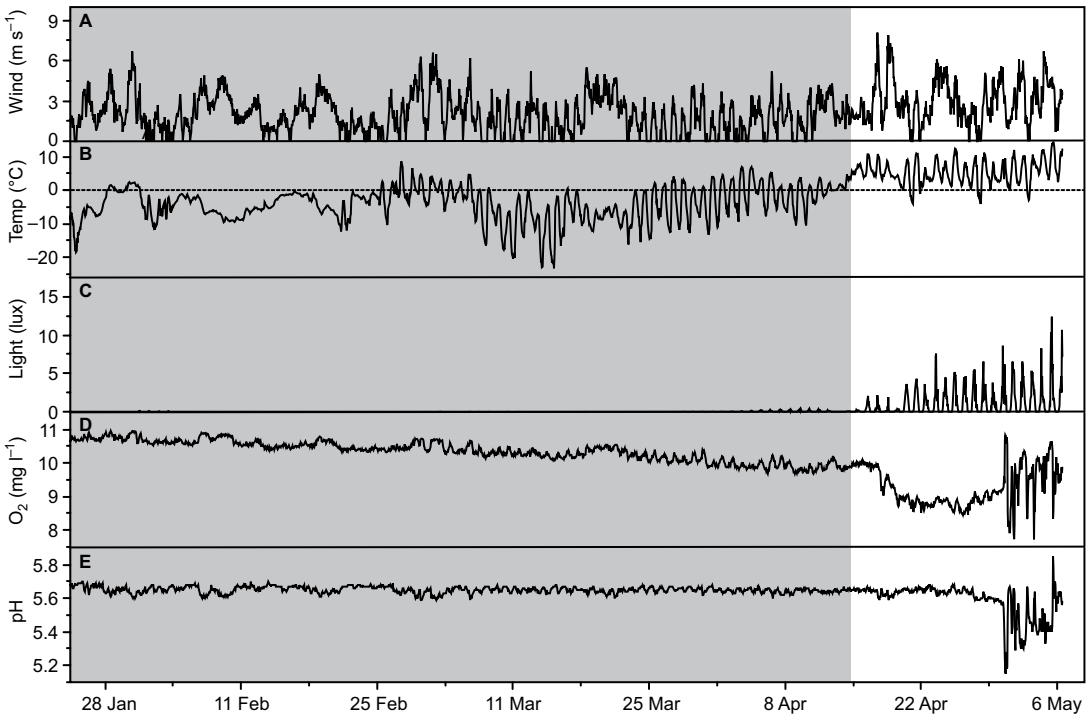

Fig. 3. (**A**) Wind speed, (**B**) ambient temperature, (**C**) light intensity at the water surface, (**D**) dissolved oxygen, and (**E**) pH measured at 4 m depth during the ice-cover (grey) and ice-melt periods (white) between 22 Jan. and 7 May 2013. The dashed line in the ambient temperature panel represents 0 °C, the freezing point of water.

CO_2 spatial variability from ice-on to ice-melt

We found that the CO_2 concentrations in the surface and bottom waters (0.5 and 8 m, respectively) at the site with the continuous CO_2 measurements (site Station in Fig. 1) differed significantly (matched pairs *t*-test result: $t = 4.1$, $p < 0.01$, number of pairs = 6). The largest difference between surface and bottom water CO_2 concentrations (181 μM) at that site occurred in May. The difference remained significant when we considered only the ice-cover period, i.e. five sampling occasions from 13 Dec. to 11 Mar. (matched pairs *t*-test result: $t = 4.2$, $p < 0.05$, number of pairs = 5). We observed that the difference in the CO_2 concentrations between the surface and bottom waters at the site Station increased below the ice cover from 18 μM on 13 Dec. to 122 μM on 11 Mar. The increase was substantially faster during early winter with mean ΔCO_2 of 1.1 μM d^{-1} in the surface water and 2.6 μM d^{-1} in the bottom water as compared with that during late winter when ΔCO_2 equaled 0.5 μM d^{-1} in the surface water and 1.2 μM d^{-1} in the bottom water. During the ice-melt period ΔCO_2 was 2.7 μM d^{-1} in the surface water and 0.2 μM d^{-1} in the bottom water.

Applying a two-way ANOVA to test the CO_2 concentration variability in the surface water across six sampling sites during the ice-cover period we found that time had a significant effect on the CO_2 variability while site had not ($F = 7.0$, $p < 0.0001$ for time and $p > 0.05$ for site, $n = 30$). Thus, the variation in the horizontal CO_2 concentration below the ice cover was insignificant in comparison with the temporal variation in the CO_2 concentration.

Whole-lake CO_2 storage from ice-on to ice-melt

During the sampled ice-cover period (13 Dec. 2012–11 Mar. 2013), whole-lake CS increased by 61% from 27 938 mol to 45 905 mol (Table 1). Whole-lake CO_2 accumulation (Eq. 1) rap-

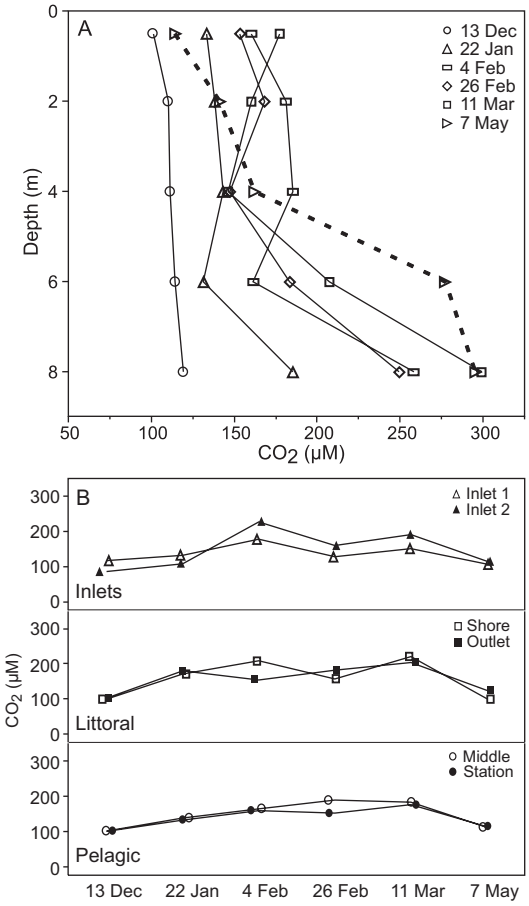

Fig. 4. (**A**) Vertical and (**B**) horizontal, surface-water CO_2 concentrations in Lake Gäddtjärn during the ice-cover period (13 Dec. 2012–11 Mar. 2013) and at ice-off (7 May 2013).

idly increased in early winter (13 Dec. 2012–4 Feb. 2013) with r = 338 mol d^{-1}. Thereafter, from 4 Feb.–11 Mar., whole-lake CO_2 storage remained relatively stable until ice-melt (r = 1.3 mol d^{-1}). During the ice-cover period (28 Nov. 2012–15 Apr. 2013), whole-lake CS increased by 50% from 22 868 mol to 45 951 mol. While during the three-week spring ice-melt period (i.e. 15 Apr.–7 May), 33% of the total whole-lake CO_2 was released, reducing CS to 30 618 mol. This whole-lake CO_2 loss was rapid with r reaching 665 mol d^{-1}. In total, 18 000–23 000 mol of CO_2 was accumulated in the lake during winter of which 15 000 mol was released at ice-melt, and 3000–8000 mol remained in the lake, mainly in the bottom waters (Fig. 4A). Thus, for the sampled period, $C_{release}$ was 85%, i.e. 85% of the total CO_2 accumulated during winter was released at ice-melt. $C_{release}$ estimated for the whole ice-cover period equalled 66%.

CO_2 emission at ice-melt

Although the spring emission of CO_2 at ice-melt has the potential to be strong, with a maximum of 88 mmol m^{-2} d^{-1}, the spring turnover was short and incomplete. During the spring CO_2-emission period (16 Apr.–4 May), the daily mean ± SD k_{600} was 2.6 ± 0.5 cm h^{-1}, and the daily mean ± SD CO_2 concentration 144 ± 23 μM, which corresponds to a daily mean CO_2 emission of 38 ± 11 mmol m^{-2} d^{-1}. During the first peak, accounting for 28%–36% of the total spring CO_2 emissions, the daily mean ± SD k_{600} equalled 2.7 ± 0.7 cm h^{-1}, the daily mean ± SD CO_2 concentration 167 ± 33 μM, and the daily mean ± SD CO_2 emission 44 ± 16 mmol m^{-2} d^{-1}. During the second peak which accounted for 64%–72% of the total spring CO_2 emissions, the daily mean ± SD k_{600} was 2.6 ± 0.4 cm h^{-1}, the daily mean ± SD CO_2 concentration 136 ± 11 μM, and the daily mean ± SD CO_2 emission 36 ± 7 mmol m^{-2} d^{-1}.

Water temperatures below the ice cover

On 13 Dec. (first sampling), the temperature difference between the bottom (8 m) and surface (0.5 m) water layers was greater than 2 °C (Fig. 5A), and this temperature difference remained similar throughout the whole ice-cover season (Fig. 5B). A similar gradient persisting during the entire ice-cover period was observed for oxygen with its content decreasing from the top to bottom waters (data not shown). The temperature difference remained unchanged between the beginning of the ice melt (15 Apr.) and 26 Apr. (Fig. 5C). Thus, water mixing began around 11 days later than the ice-melt.

Discussion

The surface-water CO_2 concentrations measured continuously at 2 m depth from ice-on to ice-off,

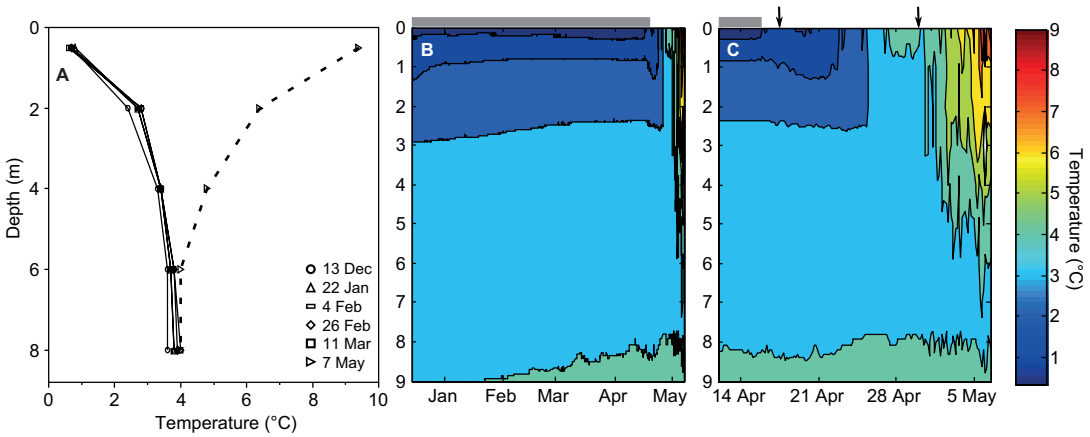

Fig. 5. Depth profile of lake-water temperatures measured during (**A**) field sampling, (**B**) ice-on to ice-melt period from 22 Jan. to 7 May. 2013, and (**C**) during spring ice-melt from 13 Apr. to 7 May. 2013. In panel **A** the dashed line represents field sampling during ice-off. In panels **B** and **C** the grey horizontal bars represent ice cover. In panel **C** the black arrows correspond to CO_2 concentration peaks 3 and 4 in Fig. 2.

showed four distinct phases (Fig. 2). Contradictory to our hypothesis and previous studies (e.g. Huotari *et al*. 2009), continuous CO_2 concentration measurements and whole-lake CO_2 storage estimates below lake ice revealed that CO_2 did not steadily increase throughout the winter (Fig. 2). Rather, CO_2 concentration and whole-lake CO_2 storage increased only in early winter but in late winter the concentrations remained relatively constant after maximum ice thickness had been reached (Table 1 and Fig. 2).

Previous studies in ice-covered lakes found lower concentrations of CO_2 under the ice in late winter, which was attributed to under-ice primary production (Baehr and DeGrandpre 2004, Huotari *et al*. 2009). However, in our lake primary production under ice was highly unlikely, as light intensity was below the detection limits (Fig. 3C) due to thick snow and ice cover (Table 1). Also Sobek *et al*. (2003) found low nutrient concentrations (total phosphorus = 10.8 μg l^{-1}, total nitrogen = 190 μg l^{-1}) and chlorophyll *a* concentrations being under the detection limit in ice-covered Lake Gäddtjärn.

Since the study lake is small, with a relatively short water residence time (~2 months), and thus substantially affected by the catchment, we suggest that catchment CO_2 inputs (surface and subsurface flow) and biological in-lake CO_2 production are the drivers of surface-water CO_2 accumulation in early winter. Similarly, Karlsson *et al*. (2013) and Striegl *et al*. (2001) found decomposition of organic matter and CO_2 inputs from the catchment to be important in early winter. Once ice reaches maximum thickness and surrounding soils freeze, water flow from the catchment to the lake is minimized, reducing catchment inputs and mixing of water masses below ice. This is indicated by the stable temperature profile during the entire ice-cover season (Fig. 5B). Dissolved organic matter in waters under ice in late winter has been suggested to have low aromaticity and represent more heavily-degraded material (Mann *et al*. 2012) indicating that substrate availability may be a limiting factor for bacterial respiration in the water column during late winter. This is likely in our lake, since bacterial respiration has been suggested to be limited by temperature and substrate availability (Pomeroy and Wiebe 2001), and surface water temperatures remain constantly low during the ice-cover period (Fig. 5B) while the amount of DOC available to bacterioplankton is decreasing during the ice-cover period (Table 1), and probably also the bioavailability of the remaining DOC is progressively reduced.

Sediments are probably an important source of CO_2 to the water column, as indicated by CO_2 increasing with water depth, and by its accumulation rates in the bottom water being higher than in the surface water (Fig. 4A), which is in line with earlier reports of sediment respiration being

the main source of CO_2 emissions from boreal lakes (Kortelainen *et al*. 2006). The sediments of Lake Gäddtjärn are organic-rich and contain ~25% organic carbon (data not shown), and thus represent an environment that is highly enriched in both substrate and nutrients for microbial growth and respiration, leading to substantial CO_2 production. Microbial respiration in sediments is positively and exponentially related to temperature (Gudasz *et al*. 2010, Bergström *et al*. 2010), hence sediment respiration can be expected to be higher in deeper parts of the lake where water temperature is higher (4–5 °C) than in surface water (1–2 °C), contributing to the observed higher CO_2 accumulation rates in the bottom waters in certain periods (Fig. 4A). The decreasing rate of whole-lake CO_2 accumulation (Table 1) may be related to increasing CO_2 concentrations in the bottom water over time (Fig. 4A), since the CO_2 concentration gradient between the sediment and water is reduced when the CO_2 concentration in bottom water increases, thereby reducing the rate of diffusion of CO_2 from the sediment to the bottom water. In other words, increasing bottom-water CO_2 limits further CO_2 diffusion from the sediment. Thus, in this small boreal lake we can divide the ice-cover period into two phases determined by the interplay between biological and physical factors. Similar was proposed by Bertilsson *et al*. (2013).

During late winter, it is likely that localized small-scale physical processes, i.e. water movements, give rise to small-scale oscillations observed in the continuous surface-water CO_2 concentration measurements, rather than biological processes. However, investigation of microbial activity (e.g. respiration rates, isotope analysis) under ice is further needed to confirm this. Nevertheless, physical processes can largely differ among lakes depending on lake morphometry (e.g. Riera *et al*. 1999). In larger and deeper lakes, large-scale physical processes (e.g. internal seiches and deep water turnover) were observed below the ice cover (Baehr and DeGrandpre 2002, and Baehr and DeGrandpre 2004, respectively). However, such processes are less likely to occur in wind-sheltered, small, moderately-shallow lakes such as ours. Hence, differences in physical processes as a result of differences in lake morphometry might explain why CO_2 accumulation below ice can show very different patterns among lakes.

This is the first study showing that two CO_2 concentration peaks can occur as ice-melt begins, resulting in two potentially distinct events of high CO_2 emission. In contrast, Baehr and DeGrandpre (2004), and Huotari *et al*. (2009) recorded only one CO_2 peak at ice-melt which they attributed to a combination of deep water mixing and net production. However, our continuous CO_2 concentration measurements revealed an unexpected initial peak in surface-water CO_2 on 17 Apr. that was not driven by bottom-water convective turnover, here indicated by temperature differences of more than 2 °C between bottom and surface waters at the time of the first CO_2 concentration peak (Fig. 5C). As ice-melt begins, cold, low-density, lateral catchment inputs of melting snow and stream water (Bengtsson 1996) can increase water column stability and thereby inhibit mixing to deeper layers (Kirillin and Terzhevik 2011). During spring thaw, snow meltwater and stream water have been shown to contain high concentrations of CO_2 (Dinsmore *et al*. 2011, Dinsmore *et al*. 2013, Wallin *et al*. 2013). Thus, we suggest that the first and highest CO_2 concentration peak during ice-melt was a result of small-scale, upper water column mixing of CO_2 transported laterally from the surrounding catchment. CO_2-rich surface and subsurface inflows and CO_2 mobilized from catchment soils by meltwater enriches littoral zones of a lake with CO_2 and organic matter which is then transported to the central part of the lake. Since this incoming water is cold it will only mix at similar temperature gradients in the upper water column of the lake. During the second CO_2 concentration peak on 30 Apr., however, convective turnover of deep waters becomes important, seen in our data as weakening in thermal stratification beginning on 26 Apr. (Fig. 5C). Thus, in addition to deep-water mixing, our study highlights the importance of lateral CO_2 transport at ice-melt, particularly in small lakes, which have relatively large littoral zones and catchment-to-lake-area ratios, and are the most common lake type worldwide (Downing *et al*. 2006). Studies that investigate lateral CO_2 transport into the lake at ice-melt are valu-

able and these measurements should be included in future studies to estimate their contribution to CO_2 emissions.

During the rapid decline in the CO_2 concentration at ice-off, the maximum CO_2 emission reached 88 mmol m^{-2} d^{-1}, and the daily mean ± SD CO_2 emission was 38 ± 11 mmol m^{-2} d^{-1}, which were comparable to the values found for a small boreal lake in Finland after ice breakup (maximum and mean ± SD of 55.6 mmol m^{-2} d^{-1} and 30.9 ± 16.7 mmol m^{-2} d^{-1}, respectively; *see* Huotari *et al*. 2009). Although maximum CO_2 emission rates from our lake can be considered high, spring turnover was incomplete due to rapid warming of surface waters. Thus, as already suggested by Miettinen *et al*. (2015), and indicated by the continuous surface-water CO_2 measurements, high CO_2 emissions at ice-melt during a year with incomplete spring turnover provide some evidence that external sources of CO_2 enter the lake at ice-melt. Further, incomplete turnover resulted in CO_2 remaining in the bottom waters of the lake (Fig. 4A), as not all of the CO_2 accumulated under ice was able to leave the lake at ice out. We estimated that during the ice-cover period (13 Dec. 2012–11 Mar. 2013), 85% of the total CO_2 accumulated below ice in the lake was released at ice-melt. This value was reduced to 66% when the whole ice-cover period (28 Nov. 2012–15 Apr. 2013) was taken into account. Either way, CO_2 remains in the lake and is not released at ice-melt, representing a non-negligible fraction of CO_2 accumulation under ice. These results indicate that the current assumption regarding CO_2 emission estimates that all CO_2 accumulated during the ice-cover period is emitted at ice-melt (e.g. Raymond *et al*. 2013) may not always be true. In our lake, 15%–34% of accumulated CO_2 remained, thus the whole-lake CO_2 storage was 3000–8000 mol higher at ice-off than it was at ice-on. Albeit, the storage of this remaining CO_2 may only be temporary, as CO_2 may be transported downstream or released to the atmosphere during autumn turnover which was shown to be strong (Bellido *et al*. 2009). Alternatively, CO_2 may be internally processed if it is consumed by phytoplankton or undergoes dark carbon fixation (Santoro *et al*. 2013). This result should be interpreted with caution as patterns can differ across lakes and years. For example, the stability of stratification and the depth of water column mixing at ice-melt have been found to vary between years (Huotari *et al*. 2009, Miettinen *et al*. 2015). Thus, future studies should measure the whole-lake CO_2 storage seasonally over many years to establish long-term patterns.

As compared with the open-water season, identified regulators of winter CO_2 accumulation, biological processes and thermal stratification, are similar. During summer, thermal stratification, and biological processes have been shown to mainly affect CO_2 distribution in the water column of lakes (Weyhenmeyer *et al*. 2012). Our results further suggest that biological processes and thermal stratification affect water-column CO_2 distribution in early and late winter, respectively. Although Schilder *et al*. (2013) found horizontal CO_2 surface water variability during the open-water season, with lower CO_2 concentrations found near-shore than in the middle of the lake, we did not find significant horizontal CO_2 surface water variability under ice (Fig. 4B). In-lake spatial variation during the ice-cover period may be lower than during the open-water season because ice cover creates a cold, dark environment in the lake which reduces variations in physical (e.g. lake mixing) and biological (e.g. metabolism) processes. Also, organic matter degradation in shallow, littoral sediments is greatly reduced at temperatures < 2 °C close to the ice (Gudasz *et al*. 2010). Whereas, during the open-water season, physical and biological processes can greatly vary within the lake (e.g. Hofmann 2013). In addition, we found that the difference in the CO_2 concentrations between the surface and bottom waters increased throughout winter with greatest variability at spring melt when CO_2 was emitted from surface waters. Since horizontal variability was low and vertical variability was large, repeated or continuous measurements at one point but at several depths may be sufficient to calculate whole-lake CO_2 accumulation during the ice-cover period.

In summary, this study showed that (1) CO_2 accumulation is not simply linear under ice, (2) CO_2 was accumulated faster in bottom waters than in surface waters, and (3) at ice-melt, a non-negligible fraction (15%–34%) of CO_2 that

was accumulated under ice was not emitted and remained stored in the bottom waters. These results provide new understanding of lake-water CO_2 distribution patterns under ice and at ice-melt and need to be taken into consideration when estimating annual CO_2 emissions. If up-scaling approaches assume that CO_2 accumulates linearly under ice and that all CO_2 accumulated during the ice-cover period leaves the lake at ice-melt, present estimates may overestimate CO_2 emissions from small, ice-covered lakes. Likewise, neglecting CO_2 at ice-melt will result in an underestimation of CO_2 emissions from small ice-covered lakes. Comparative studies are further needed to advance our understanding of difference in CO_2 accumulation patterns across lake type and region. How much changes in the duration of the ice-cover period in a warmer climate will affect the balance between winter CO_2 accumulation and spring CO_2 outburst remains to be studied.

Acknowledgements: Financial support was received from the NordForsk approved Nordic Centre of Excellence "CRAICC", the Swedish Research Council (VR) and the Swedish Research Council for Environment, Agricultural Sciences and Spatial Planning (FORMAS). This work is part of and profited from the networks financed by NordForsk (DOMQUA), Norwegian Research Council (Norklima ECCO), US National Science Foundation (GLEON) and the European Union (Netlake). We thank Marie-Eve Ferland for providing lake contour maps and Jan Johansson and numerous others at Uppsala University limnology group for assistance in the field. We would also like to thank two anonymous reviewers.

References

Aufdenkampe A.K., Mayorga E., Raymond P.A., Melack J.M., Doney S.C., Alin S.R., Aalto R.E. & Yoo K. 2011. Riverine coupling of biogeochemical cycles between land, oceans, and atmosphere. *Frontiers in Ecology and the Environment* 9: 53–60.

Baehr M.M. & DeGrandpre M.D. 2002. Under-ice CO_2 and O_2 variability in a freshwater lake. *Biogeochemistry* 61: 95–113.

Baehr M.M. & DeGrandpre M.D. 2004. In situ pCO_2 and O_2 measurements in a lake during turnover and stratification: observations and modeling. *Limnology and Oceanography* 49: 330–340.

Battin T.J., Luyssaert S., Kaplan L.A., Aufdenkampe A.K., Richter A. & Tranvik L.J. 2009. The boundless carbon cycle. *Nature Geoscience* 2: 598–600.

Bellido J.L., Tulonen T., Kankaala P. & Ojala A. 2009. CO_2 and CH_4 fluxes during spring and autumn mixing periods in a boreal lake (Pääjärvi, southern Finland). *Journal of Geophysical Research-Biogeosciences* 114: G04007, doi: 04010.01029/02009JG000923.

Belzile C., Vincent W.F., Gibson J.A.E. & Hove P.V. 2001. Bio-optical characteristics of the snow, ice, and water column of a perennially ice-covered lake in the High Arctic. *Canadian Journal of Fisheries and Aquatic Sciences* 58: 2405–2418.

Bengtsson L. 1996. Mixing in ice-covered lakes. *Hydrobiologia* 322: 91–97.

Bergström I., Kortelainen P., Sarvala J. & Salonen K. 2010. Effect of temperature and sediment properties on benthic CO_2 production in an oligotrophic boreal lake. *Freshwater Biology* 55: 1747–1757.

Bertilsson S., Burgin A., Carey C.C., Fey S.B., Grossart H.P., Grubisic L.M., Jones I.D., Kirillin G., Lennon J.T., Shade A. & Smyth R.L. 2013. The under-ice microbiome of seasonally frozen lakes. *Limnology and Oceanography* 58: 1998–2012.

Butman D. & Raymond P.A. 2011. Significant efflux of carbon dioxide from streams and rivers in the United States. *Nature Geoscience* 4: 839–842.

Cole J.J. & Caraco N.F. 1998. Atmospheric exchange of carbon dioxide in a low-wind oligotrophic lake measured by the addition of SF6. *Limnology and Oceanography* 43: 647–656.

Cole J.J., Caraco N.F., Kling G.W. & Kratz T.K. 1994. Carbon dioxide supersaturation in the surface waters of lakes. *Science* 265: 1568–1570.

Cole J.J., Prairie Y.T., Caraco N.F., McDowell W.H., Tranvik L.J., Striegl R.G., Duarte C.M., Kortelainen P., Downing J.A., Middelburg J.J. & Melack J. 2007. Plumbing the global carbon cycle: Integrating inland waters into the terrestrial carbon budget. *Ecosystems* 10: 172–185.

Demarty M., Bastien J. & Tremblay A. 2011. Annual follow-up of gross diffusive carbon dioxide and methane emissions from a boreal reservoir and two nearby lakes in Québec, Canada. *Biogeosciences* 8: 41–53.

Dinsmore K.J., Billett M.F., Dyson K.E., Harvey F., Thomson A.M., Piirainen S. & Kortelainen P. 2011. Stream water hydrochemistry as an indicator of carbon flow paths in Finnish peatland catchments during a spring snowmelt event. *Science of the Total Environment* 409: 4858–4867.

Dinsmore K.J., Wallin M.B., Johnson M.S., Billett M.F., Bishop K., Pumpanen J. & Ojala A. 2013. Contrasting CO_2 concentration discharge dynamics in headwater streams: A multi-catchment comparison. *Journal of Geophysical Research, Biogeosciences* 118: 445–461.

Downing J.A., Prairie Y.T., Cole J.J., Duarte C.M., Tranvik L.J., Striegl R.G., McDowell W.H., Kortelainen P., Caraco N.F., Melack J.M. & Middelburg J.J. 2006. The global abundance and size distribution of lakes, ponds, and impoundments. *Limnology and Oceanography* 51: 2388–2397.

Gudasz C., Bastviken D., Steger K., Premke K., Sobek S. & Tranvik L.J. 2010. Temperature-controlled organic carbon mineralization in lake sediments. *Nature* 466:

478–481.

Gunn J. & Keller W. 1985. Effects of ice and snow cover on the chemistry of nearshore lake water during spring melt. *Annals of Glaciology* 7: 208–212.

Hofmann H. 2013. Spatiotemporal distribution patterns of dissolved methane in lakes: how accurate are the current estimations of the diffusive flux path? *Geophysical Research Letters* 40: 2779–2784.

Huotari J., Ojala A., Peltomaa E., Pumpanen J., Hari P. & Vesala T. 2009. Temporal variations in surface water CO_2 concentration in a boreal humic lake based on high-frequency measurements. *Boreal Environment Research* 14: 48–60.

Jähne B., Heinz G. & Dietrich W. 1987. Measurements of the diffusion coefficients of sparingly soluble gases in water. *Journal of Geophysical Research* 92: 10767–10776.

Johnson M.S., Billett M.F., Dinsmore K.J., Wallin M., Dyson K.E. & Jassal R.S. 2010. Direct and continuous measurement of dissolved carbon dioxide in freshwater aquatic systems-method and applications. *Ecohydrology* 3: 68–78.

Karlsson J., Ask J. & Jansson M. 2008. Winter respiration of allochthonous and autochthonous organic carbon in a subarctic clear-water lake. *Limnology and Oceanography* 53: 948–954.

Karlsson J., Giesler R., Persson J. & Lundin E. 2013. High emission of carbon dioxide and methane during ice thaw in high latitude lakes. *Geophysical Research Letters* 40: 1123–1127.

Kirillin G. & Terzhevik A. 2011. Thermal instability in freshwater lakes under ice: Effect of salt gradients or solar radiation? *Cold Regions Science and Technology* 65: 184–190.

Kokic J., Wallin M., Chmiel H.E., Denfeld B.A. & Sobek S. 2015. Carbon dioxide evasion from headwater systems strongly contributes to the total export of carbon from a small boreal lake catchment. *Journal of Geophysical Research, Biogeosciences* 120: 13–28.

Kortelainen P., Rantakari M., Huttunen J.T., Mattsson T., Alm J., Juutinen S., Larmola T., Silvola J. & Martikainen P.J. 2006. Sediment respiration and lake trophic state are important predictors of large CO_2 evasion from small boreal lakes. *Global Change Biology* 12: 1554–1567.

Krenz J. 2013. *Measuring CO_2 emissions from a small boreal lake and its connecting streams using automatic floating chambers*. Swedish University of Agriculture Sciences, Uppsala.

Mann P.J., Davydova A., Zimov N., Spencer R.G.M., Davydov S., Bulygina E., Zimov S. & Holmes R.M. 2012. Controls on the composition and lability of dissolved organic matter in Siberia's Kolyma River basin. *Journal of Geophysical Research* 117: G01028, doi:01010.01029/02011JG001798.

Michmerhuizen C.M., Striegl R.G. & McDonald M.E. 1996. Potential methane emission from north-temperate lakes following ice melt. *Limnology and Oceanography* 41: 985–991.

Miettinen H., Pumpanen J., Heiskanen J.J., Aaltonen H., Mammarella I., Ojala A., Levula J. & Rantakari M. 2015. Towards a more comprehensive understanding of lacustrine greenhouse gas dynamics — two-year measurements of concentrations and fluxes of CO_2, CH_4 and N_2O in a typical boreal lake surrounded by managed forests. *Boreal Environment Research* 20: 75–89.

Pomeroy L.R. & Wiebe W.J. 2001. Temperature and substrates as interactive limiting factors for marine heterotrophic bacteria. *Aquatic Microbial Ecology* 23: 187–204.

Raymond P.A., Hartmann J., Lauerwald R., Sobek S., McDonald C., Hoover M., Butman D., Striegl R., Mayorga E., Humborg C., Kortelainen P., Durr H., Meybeck M., Ciais P. & Guth P. 2013. Global carbon dioxide emissions from inland waters. *Nature* 503: 355–359.

Riera J.L., Schindler J.E. & Kratz T.K. 1999. Seasonal dynamics of carbon dioxide and methane in two clear-water lakes and two bog lakes in northern Wisconsin, USA. *Canadian Journal of Fisheries and Aquatic Sciences* 56: 265–274.

Rouse W.R., Oswald C.J., Binyamin J., Spence C.R., Schertzer W.M., Blanken P.D., Bussieres N. & Duguay C.R. 2005. The role of northern lakes in a regional energy balance. *Journal of Hydrometeorology* 6: 291–305.

Santoro A.L., Bastviken D., Gudasz C., Tranvik L. & Enrich-Prast A. 2013. Dark carbon fixation: an important process in lake sediments. *PloS ONE* 8: e65813, doi:65810.61371/journal.pone.0065813.

Schilder J., Bastviken D., van Hardenbroek M., Kankaala P., Rinta P., Stotter T. & Heiri O. 2013. Spatial heterogeneity and lake morphology affect diffusive greenhouse gas emission estimates of lakes. *Geophysical Research Letters* 40: 5752–5756.

Sellers P., Hesslein R.H. & Kelly C.A. 1995. Continous measurement of CO_2 for estimation of air–water fluxes in lakes: An in situ technique *Limnology and Oceanography* 40: 575–581.

Sobek S., Algesten G., Bergstrom A.K., Jansson M. & Tranvik L.J. 2003. The catchment and climate regulation of pCO_2 in boreal lakes. *Global Change Biology* 9: 630–641.

Striegl R.G. & Michmerhuizen C.M. 1998. Hydrologic influence on methane and carbon dioxide dynamics at two north-central minnesota lakes. *Limnology and Oceanography* 43: 1519–1529.

Striegl R.G., Kortelainen P., Chanton J.P., Wickland K.P., Bugna G.C. & Rantakari M. 2001. Carbon dioxide partial pressure and ^{13}C content of north temperate and boreal lakes at spring ice melt. *Limnology and Oceanography* 46: 941–945.

Tranvik L.J., Downing J.A., Cotner J.B., Loiselle S.A., Striegl R.G., Ballatore T.J., Dillon P., Finlay K., Fortino K., Knoll L.B., Kortelainen P.L., Kutser T., Larsen S., Laurion I., Leech D.M., McCallister S.L., McKnight D.M., Melack J.M., Overholt E., Porter J.A., Prairie Y., Renwick W.H., Roland F., Sherman B.S., Schindler D.W., Sobek S., Tremblay A., Vanni M.J., Verschoor A.M., von Wachenfeldt E. & Weyhenmeyer G.A. 2009. Lakes and reservoirs as regulators of carbon cycling and climate. *Limnology and Oceanography* 54: 2298–2314.

Wallin M.B., Grabs T., Buffam I., Laudon H., Agren A., Oquist M.G. & Bishop K. 2013. Evasion of CO_2 from streams — the dominant component of the carbon export

through the aquatic conduit in a boreal landscape. *Global Change Biology* 19: 785–797.

Weiss R.F. 1974. Carbon dioxide in water and seawater: the solubility of a non-ideal gas. *Marine Chemistry* 2: 203–215.

Weyhenmeyer G.A., Kortelainen P., Sobek S., Müller R. & Rantakari M. 2012. Carbon dioxide in boreal surface waters: a comparison of lakes and streams. *Ecosystems* 15: 1295–1307.

Weyhenmeyer G.A., Livingstone D.M., Meili M., Jensen O., Benson B. & Magnuson J.J. 2011. Large geographical differences in the sensitivity of ice-covered lakes and rivers in the northern hemisphere to temperature changes. *Global Change Biology* 17: 268–275.